Ethene

7.1 Introduction

In the field of electrical properties, ethene is a molecule for which there has been substantial theoretical and experimental interest. Mean polarizability measurements have been reported, with older refractivity measurements [1-3] and some more recent measurements available [4, 5]. The polarizability tensor and polarizability anisotropy have also been studied via Rayleigh light scattering [6-9], Kerr effect measurements [10, 11], Stark effect [12] and pure rotational Raman spectroscopy [13]. A very recent determination of the molecular quadrupole moment via the Zeeman effect of 1,1-dideuteroethene has been published [14].

Due to the abundance of experimental data for this molecule, ethene is considered an ideal candidate for a theoretical electrical properties study that incorporates vibrational and thermal corrections into the predicted properties. The majority of earlier theoretical studies on the electrical properties of ethene have been summarised by Maroulis [15, 16]. Vibrational corrections to the electrical properties have been calculated at the SCF level by Martí *et al.* [17] but a detailed comparison of theory with experiment was not undertaken. The present Chapter seeks to demonstrate the accuracy attainable via *ab initio* methods if zero-point vibrational corrections (ZPVCs) are combined with high-level theoretical predictions. Pure vibrational polarizabilities, thermal corrections and the effects of deuterium substitution on electrical properties are also investigated. As with previous Chapters, a detailed comparison of theory with experiment is presented with an emphasis on resolving any discrepancies between the present predictions and accurate experimental estimates.

7.2 Computational methods

The SCF and MP2 vibrational calculations were carried out using the least-squares method to obtain the necessary energy and property derivatives, as previously outlined in Chapter 3. Symmetry was extensively utilised to reduce the total number of displaced geometry calculations required using the standard quartic grid from 361 to 175 displaced geometries at which to perform energy and property calculations for each level of theory. Resonance treatment was also incorporated into the calculations with a Fermi resonance tolerance of 200 cm^{-1} applied to the vibrational calculations.

Four basis sets have been used in the present Chapter and exponents and contraction coefficients are supplied in Appendix IV. The DZP–ANO2 [$5s3p2d/3s2p$] basis set, previously used for the fluoromethanes study in Chapter 6, has been utilised for the vibrational calculations. The DZP–ANO2(f) [$5s3p2d1f/3s2p$] and DZP–ANO3 [$5s3p3d/3s2p$] respectively were used for more accurate quadrupole moment and polarizability predictions. Another basis set formed by adding d-type functions to H for the DZP–ANO3 basis set with an exponent of 0.4 was constructed, termed DZP–ANO3–H(d) [$5s3p3d/3s2p1d$], and this set was used exclusively for accurate polarizability calculations. Electrical property calculations were carried out at the Martin, Lee and Taylor CCSD(T) best estimated theoretical r_e geometry (r_{cc} = 1.3307(3) Å, r_{CH} = 1.0809(3) Å, θ_{CCH} = 121.44(3) °) [18] using finite-field and finite-field-gradient techniques with field strengths of 0.001 au and field-gradient strengths of 0.0005 au. Numerical errors in the mean polarizability and quadrupole moment are expected to be less than 0.001 au and 0.0005 au respectively.

7.3 Results and discussion

7.3.1 Zero-point vibrational corrections

Examining the ZPVCs to ethene, displayed in Table 7.1, it is apparent that although the MP2 correction to the xx component of the quadrupole moment is in reasonable agreement with the SCF value, the effects of vibration on the yy and zz components are quite different at SCF and MP2 levels. For the MP2 level of theory, the xx and yy components are of similar magnitude but opposite in sign, and the contribution to Θ_{zz} is negligible. The quadrupole moments are also decreased in magnitude with the addition of the vibrational corrections. It is difficult to develop a simple atomic charge model, for individual quadrupole moment tensor components, to rationalise particular vibrations that most affect the quadrupole moment since $\Theta_{\alpha\beta}$ is defined as a linear combination of second moment components. Investigations of the vibrational contributions to the second moments for

asymmetric top molecules may be more informative. Nevertheless, the vibrations that most affect the quadrupole moments are generally those which involve a distortion of the molecular plane. Large contributions to Θ_{xx} arise from the CH_2–CH_2 twist, antisymmetric and symmetric wags; antisymmetric and symmetric out-of-plane vibrations, in conjunction with the C–C stretch, most strongly affect the *yy* component of the quadrupole moment.

Turning to the polarizability tensor corrections, it may be observed that with the exception of the *zz* component, both SCF and MP2 ZPVCs are in fine agreement. Percentage corrections to the mean polarizabilities are 3.8 and 3.3% respectively for SCF and MP2. Polarizability anisotropy corrections which depend on the equilibrium properties are found to be relatively large with 6.1 and 4.7% corrections for SCF and MP2 levels of theory respectively. Martí *et al.* [17] have presented SCF vibrational corrections and pure vibrational polarizabilities for ethene. Although a TZ2P basis was utilised in that work, the polarization functions are not diffuse enough to guarantee accurate polarizabilities. Nevertheless, their corrections are reasonably close to the present SCF results and this would suggest that less polarized basis sets may still yield reliable ZPVCs.

Calculated thermal corrections from equation (2.71) at 300 K, $\langle P \rangle^{300\ K} - \langle P \rangle_0$, to the quadrupole moment tensor at the MP2 level of theory have been found to be extremely small with values of (−0.0017, 0.0015, 0.0002 au) obtained for (Θ_{xx}, Θ_{yy}, Θ_{zz}). For the polarizability tensor, thermal corrections of (0.0020, 0.0031, 0.0050 au) for (α_{xx}, α_{yy}, α_{zz}) tensor components have been computed. As the thermal contributions are exceedingly small with respect to the property ZPVCs, they have been neglected from the accurate theoretical predictions (in Section 7.3.3) for comparison with experimental results.

Table 7.1.

SCF and MP2 DZP–ANO2 vibrationless properties and zero-point vibrational corrections (in au) to the electrical properties of ethene.[a]

Property	SCF		MP2	
	P_e	ZPVC	P_e	ZPVC
Θ_{xx}	1.2399	−0.03600	1.2332	−0.03972
Θ_{yy}	−2.8419	0.01903	−2.5988	0.04033
Θ_{zz}	1.6020	0.01697	1.3656	−0.00061
α_{xx}	24.3228	1.1420	25.5573	1.1729
α_{yy}	22.4867	0.4628	22.9239	0.4395
α_{zz}	36.1382	1.5032	34.8341	1.1728
α	27.6492	1.0360	27.7718	0.9284
$\Delta\alpha$	12.8324	0.7774	10.8362	0.5051

[a] The principal rotation axis was chosen to be the z axis with the molecule in the xz plane. Quadrupole moment corrections refer to centre of mass coordinates with vibrationless properties P_e calculated at the respective SCF and MP2 optimized geometries (reported in Appendix III).

The vibrational mode contributions to the mean polarizability from the MP2/DZP–ANO2 A term coefficients (equation (2.39)) are reported in Table 7.2. The mode types for the molecule supplied in the table are from Herzberg [19]. The vibrational modes that most affect the mean polarizability are the high frequency C–H stretches since these effectively increase the molecular size of the molecule. Large amplitude (low frequency) vibrational modes that involve wagging and out-of-plane motions do not strongly affect the mean polarizability but greatly influence $\Theta_{\alpha\beta}$ as mentioned previously.

Table 7.2.

Vibrational A term coefficients for the mean polarizability of ethene.[a]

Mode i	ω_i	A_i	Mode Type
5	3277.4	0.3116	trans C–H stretch
1	3208.2	0.2941	symm. C–H stretch
9	3304.4	0.2786	cis C–H stretch
11	3191.1	0.2772	antisymm. C–H stretch
2	1652.3	0.1357	C–C stretch
4	1049.0	0.1052	H_2C–CH_2 twist
3	1369.8	0.0907	symm. HCH bend
12	1481.5	0.0897	antisymm. HCH bend
6	1251.2	0.0725	antisymm. HCH wag
8	971.7	0.0705	antisymm. out-of-plane
7	976.8	0.0587	symm. out-of-plane
10	831.8	0.0405	symm. HCH wag

[a] All A term coefficients (see equations (2.34) and (2.39)) are in atomic units and harmonic vibrational frequencies, ω_i, are in cm^{-1}. Vibrational modes and their descriptions are from Herzberg [19].

7.3.2 *Pure vibrational polarizabilities*

Pure vibrational polarizabilities are presented in Table 7.2, with the most accurate MP2 predictions in accord with experimental values from Nakanaga *et al.* [20] and lying within the estimated uncertainties for both the yy and zz components. Agreement between theoretical SCF and MP2 components and experiment is generally quite satisfactory. Experimental estimates of the pure vibrational polarizability from an older source [21] are also reported in Table 7.2. It seems that the associated uncertainties are overly optimistic and the errors of Nakanaga *et al.* [20] perhaps offer a more realistic indication of the true accuracy of the measurements. The infrared intensity values of Jalsovszky and Pulay [22] for the v_7 band (949.2 cm^{-1}) used in the compilation of Bishop and Cheung [23] appear to be inaccurate since their intensity of 20.3 km mol^{-1} is much larger than both an MP2/DZP–ANO2 value of 0.0385 km mol^{-1} for a harmonic intensity calculation and the experimental estimate of Nakanaga *et al.* of 0.03 km mol^{-1}.

Table 7.2.

SCF and MP2 DZP–ANO2 ground state pure vibrational
polarizabilities (in au) for ethene.[a]

	SCF	MP2	Experiment
α_{xx}^v	0.079	0.057	0.074(7)[b], 0.092(5)[c]
α_{yy}^v	2.706	2.639	2.54(10), 2.442(2)
α_{zz}^v	0.257	0.184	0.18(2), 0.168(8)
α^v	1.014	0.960	0.93(3), 0.900(3)

[a] See footnote (a) Table 7.1 for molecular orientation.

[b] Derived from experimental infrared intensities [20].

[c] Derived from experimental infrared intensities using the supplied error estimates [21].

7.3.3 *Critical comparison of theory with experiment*

Although a number of other theoretical studies have been performed on ethene, the present theoretical results are not directly compared with other theoretical work. Instead, the reader is directed to two theoretical studies by Maroulis [15, 16] that conveniently summarise the majority of theoretical calculations on the quadrupole moment and polarizability tensor. As in earlier Chapters in this thesis, the present results are compared directly, and critically, with experiment.

Examining the DZP–ANO3 polarizabilities for various levels of theory in Table 7.3, most electron correlation treatments that include the effects of linked triple excitations give quite accurate predictions of α and $\Delta\alpha$ after vibrational corrections have been applied. The MP4, MP4(Feenberg), QCISD(T) and BD(T) levels of theory all include perturbative triple excitations and the resulting polarizability predictions are quite close to experiments although the MP4 methods produce slight overestimates when compared to the CCSD based approaches. As expected, the MP4-SDQ, QCISD and BD methods for treatment of electron correlation yield smaller values of α and typically larger values of $\Delta\alpha$ than those obtained from the more complete MP4, QCISD(T) and BD(T) procedures.

The present most accurate vibrationally averaged theoretical predictions for the electrical properties are presented in Table 7.4 where the DZP–ANO2(f) and DZP–ANO3–H(d) molecular basis sets have been used for calculation of the vibrationless quadrupole moment and polarizabilities respectively. Accurate theoretical BD(T) estimates of the quadrupole moment tensor are found to agree well with a recent experimental determination from the molecular Zeeman effect study on 1,1-dideuteroethene [14]. The zz component from the current BD(T) estimate is virtually identical to the experimental value. Theoretical xx and yy components are within 4.9 and 1.7% respectively of experiment which must be considered extremely good. Improvements in the treatment of electron correlation generally decrease the magnitude of all components of the quadrupole moment tensor. Other quadrupole moment experiments have been carried out and are conveniently summarised in Maroulis [15]. Quadrupole moment experimental values in best agreement with present results include the collision induced absorption result from Dagg *et al.* [24] with values of (1.15, −2.32, 1.17 au) for (xx, yy, zz) components. A molecular Zeeman effect experimental estimate of the quadrupole moment tensor has been reported by Kukolich *et al.* [25] for the ethene-HCl complex with the values (1.04, −2.45, 1.63 au). The accuracy of these measurements is probably affected by the indirect nature of the observations and the

approximations utilised. However, with the exception of the zz component, agreement with present BD(T) estimates is quite satisfactory.

Considering the static mean polarizabilities in Table 7.4, the experimental work of Hohm [4] is judged the most reliable with the BD(T) vibrationally averaged estimate lying within just 0.13% of the static experimental estimate. Jhanwar *et al.* [5] have published a value of 27.70 au which is also in fine agreement with the present theoretical values. A recent Kerr effect study has been carried out on this molecule by Tammer and Hüttner [11] and the present theoretical tensor components lie close to their corresponding experimental static estimates. Other experimental results for the polarizabilities, reported in Table 7.3, are quite reliable when the underlying frequency dependence of some of the measurements is taken in account. Tensor components from the pure rotational Raman effect measurements use a value of the depolarization ratio at 632.8 nm from Bridge and Buckingham [8] and therefore the experimentally derived tensor components correspond to this wavelength. Tensor components from the Stark effect [12] should be directly comparable to the present theoretical static values but are less accurate than the other experiments. The present theoretical value of 11.41 au for $\Delta\alpha$ (Table 7.4) compares favorably with the static experimental estimates of 11.45(23) [7] and 11.45(5) au [6] from extrapolation of Rayleigh light scattering data.

Table 7.3.
Vibrationally averaged polarizabilities (in au) for ethene.[a]

Level of Theory	α_{xx}	α_{yy}	α_{zz}	α	$\Delta\alpha$
SCF	25.614	23.142	37.940	28.899	13.730
MP2	26.263	22.865	35.274	28.134	11.107
MP3	25.902	22.306	34.918	27.709	11.253
MP4-SDQ	25.838	22.113	34.999	27.650	11.486
MP4	26.116	22.440	35.104	27.887	11.284
MP4(Feenberg)	26.123	22.409	35.136	27.889	11.336
QCISD	25.816	22.109	35.141	27.689	11.631
QCISD(T)	26.023	22.286	35.056	27.788	11.372
BD	25.787	22.109	34.988	27.628	11.490
BD(T)	26.018	22.301	35.022	27.780	11.329
Experimental					
	26.02(24)[b]	22.38(18)	35.06(12)	27.800(12)[c] 27.70[f]	11.45(23)[d] 11.45(5)[g]
	26.1[e]	22.9	36.4		
	24.6[h]	24.2	37.3	27.8(14)	14.2(7)

[a] Vibrationless property calculations were carried out at the theoretical CCSD(T) geometry [18] using the DZP–ANO3 basis set. SCF/DZP–ANO2 ZPVCs have been applied to SCF/DZP–ANO3 property calculations; MP2/DZP–ANO2 ZPVCs have been applied to DZP–ANO3 properties for correlated levels of theory.

[b] Static polarizability tensor components from the Kerr effect [11].

[c] Static estimate from a quadratic extrapolation of polarizability data (five wavelengths between 633 and 325 nm) [4].

[d] Static estimate from two-point extrapolation of $\Delta\alpha(\omega_\sigma)$ from Rayleigh depolarization ratios [7] combined with dynamic mean polarizabilities [4].

[e] Dynamic 632.8 nm polarizability tensor components from a combination of Rayleigh depolarization ratios [8], rotational Raman effect measurements and a 632.8 nm estimate of the mean polarizability from refractivity data [13].

[f] DOSD static estimate [5].

[g] Static estimate from an extrapolation to zero frequency of $\Delta\alpha(\omega_\sigma)$, obtained from Rayleigh depolarization ratios [6] combined with dynamic mean polarizabilities [4].

[h] Static polarizability tensor components, mean polarizability and polarizability anisotropy from Stark effect measurements for the ground vibrational state [12].

Table 7.4.
Vibrationally averaged quadrupole moments, polarizabilities and polarizability
anisotropies (in au) for ethene.[a]

Property	Level of Theory				
	SCF	MP2	BD	BD(T)	Experiment
Θ_{xx}	1.2345	1.1756	1.1487	1.1494	1.10(7)[b]
Θ_{yy}	−2.8051	−2.4904	−2.4223	−2.3909	−2.35(14)
Θ_{zz}	1.5706	1.3149	1.2736	1.2415	1.24(14)
α_{xx}	25.636	26.335	25.841	26.081	26.02(24)[c]
α_{yy}	23.128	22.866	22.127	22.314	22.38(18)
α_{zz}	37.956	35.385	35.103	35.134	35.06(12)
α	28.907	28.195	27.691	27.843	27.800(12)[d], 27.70[e]
$\Delta\alpha$	13.747	11.195	11.575	11.412	11.45(23)[f], 11.45(5)[g]

[a] DZP–ANO2 vibrational corrections have been applied to property calculations at the theoretical CCSD(T) geometry using the DZP–ANO3–H(d) basis for polarizabilities and the DZP–ANO2 (f) for the quadrupole moment (See text). SCF ZPVCs have been applied to SCF property calculations; MP2 ZPVCs have been applied to properties from correlated levels of theory. Quadrupole moments refer to centre of mass coordinates.

[b] Rotational Zeeman effect for 1,1-dideuteroethene (CH_2CD_2) at 101 K [14].

[c] Static polarizability tensor components from the Kerr effect [11].

[d] Static estimate from a quadratic extrapolation of polarizability data (five wavelengths between 633 and 325 nm) [4].

[e] DOSD static estimate [5].

[f] Static estimate from two-point extrapolation of $\Delta\alpha(\omega_\sigma)$ from Rayleigh depolarization ratios [7] combined with dynamic mean polarizabilities [4].

[g] Static estimate from an extrapolation to zero frequency of $\Delta\alpha(\omega_\sigma)$, obtained from Rayleigh depolarization ratios [6] combined with dynamic mean polarizabilities [4].

7.3.4 *Properties of CH_2CD_2 and C_2D_4*

As part of the investigation for ethene, the effect of isotopic substitution of deuterium on the electrical properties of 1,1-dideuteroethene and perdeuteroethene is studied. The molecular Zeeman effect quadrupole moment determination by Majer *et al.* [14] was performed for CH_2CD_2 and so it would be gratifying to be able to validate the accuracy of this measurement through computation of the effects of zero-point vibrational motion for the quadrupole moment. Dideuteroethene also possesses a vibrationally induced dipole moment that has been experimentally determined [26] via the second-order Stark effect.

Utilising the internal coordinates definition from Lee *et al.* [27] and non-linear **L** tensor transformations of cubic property derivatives and quartic energy derivatives, as described in Chapters 2 and 3, MP2/DZP-ANO2 zero-point vibrational properties have been calculated and are displayed in Table 7.5. Fourth-order property derivatives have been excluded from the transformations due to the lack of formulae for the fourth-order **L** tensor torsional derivatives required for the full non-linear transformation. Deletion of fourth-order property derivatives from the complete ZPVCs reduces the magnitude of most corrections, denoted ZPVC($-P_4$) in Table 7.5, but the effect is small, amounting to removal of a small percentage of a relatively small vibrational correction. The resulting vibrationally induced ground state dipole moment for CH_2CD_2 of 0.003270 au compares well with an experimentally measured value from Hirota *et al.* of 0.0036(2) au [26]. It is expected that the theoretical value is an underestimate as fourth-order dipole moment derivatives have not been included in the computed value. To date, no theoretical predictions of this property have been forwarded so the present values represent the first of their kind for CH_2CD_2. Differences between ZPVCs to the quadrupole moment tensor of CH_2CD_2 and C_2H_4 are exceedingly small, far smaller than the experimental uncertainties, thus supporting the transferability (between these isotopomers) for the experimentally determined quadrupole moment [14]. Isotopic substitution generally decreases the amplitudes of the vibrational modes leading to property ZPVCs of the deuterated isotopomers that are correspondingly smaller than those of the parent molecule. The deuterium isotopic difference, ZPVC(C_2H_4) − ZPVC(C_2D_4), for the static mean polarizability is quite large and may be amenable to measurement via accurate refractivity or polarizability experiments. An isotopic difference for $\Delta\alpha$ is dependent on the vibrationless polarizability tensor and has not been presented in Table 7.5 in an attempt to avert possible confusion (See Chapter 2, Section 2.4). Using the present BD(T)/DZP–ANO3–H(d) estimates of the polarizability tensor, the deuterium isotopic difference to $\Delta\alpha$ of ethene is calculated to be 0.1386 au. This quantity may be measurable using extremely accurate Rayleigh depolarization experiments.

Table 7.5.

MP2 DZP–ANO2 zero-point vibrational corrections (in au) to the electrical
properties of ethene, 1,1-dideuteroethene and perdeuteroethene.[a]

| Property | CH$_2$CH$_2$ | | CH$_2$CD$_2$ | CD$_2$CD$_2$ |
	ZPVC	ZPVC($-P_4$)	ZPVC($-P_4$)	ZPVC($-P_4$)
Θ_{xx}	−0.03972	−0.02749	−0.02333	−0.01911
Θ_{yy}	0.04033	0.03587	0.03117	0.02601
Θ_{zz}	−0.00061	−0.00838	−0.00783	−0.00690
α_{xx}	1.1729	1.1642	1.0166	0.8700
α_{yy}	0.4395	0.4005	0.3594	0.3167
α_{zz}	1.1728	1.1681	1.0287	0.8871
α	0.9284	0.9109	0.8016	0.6913

[a] Quadrupole moment corrections were derived from quadrupole moments relative
to the centre of mass. ZPVC($-P_4$) refers to a zero-point vibrational correction
calculated by setting all fourth-order property derivatives of μ_α, $\Theta_{\alpha\beta}$, and
$\alpha_{\alpha\beta}$ to zero in the relevant perturbation theory expressions.

7.3.5 *Frequency dependence of the dipole polarizability tensor*

In order to fully assess the accuracy of the available Rayleigh light scattering measurements, it is necessary to investigate the frequency dependence of the polarizability tensor. For this purpose, pseudo-BD(T) polarizability tensors were calculated at six optical wavelengths using the method outlined in Chapter 3. Armed with this information, mean polarizabilities and Rayleigh depolarization ratios have been calculated and plotted with experimental values in Figures 7.1 and 7.2. Present theoretical pseudo-BD(T) mean polarizabilities are typically within 1% of the dynamic polarizability measurements of Hohm [4]. For the depolarization ratio of ethene, the agreement between theory and experiment is excellent with theory lying within 2% of the results of Bogaard, Buckingham, Pierens and White (BBPW) [6] and Baas and van den Hout [7] for the measurements at 632.8 nm and 514.5 nm. Extrapolated estimates converge to the same static value which is gratifying as improvements in basis set are likely to lead to a slightly larger depolarization ratio at zero frequency, in perfect match with the experimental curve of BBPW [6]. Measurements of Bridge and Buckingham [8] and a recent estimate from Couling and Graham [9] also support the BBPW results. Fine agreement between theory and experiment is obtained for ρ_0 and this is most likely due to the relatively large depolarization ratio for ethene. For molecules with small depolarization ratios, such as the fluoromethanes (Chapter 6) and H_2S (Chapter 5), the vibrational Raman contribution can markedly affect both the frequency dependence and magnitude of the observed depolarization ratio. However, if the depolarization ratio is large, then the relative percentage contribution from the vibrational Raman effect is expected to be small for common laser wavelengths. Although the magnitude of the vibrational Raman contribution cannot be definitively established without further theoretical and experimental work, the agreement between theory and experiment in Figure 8.2 would imply that the vibrational Raman contribution to ρ_0 is small for ethene.
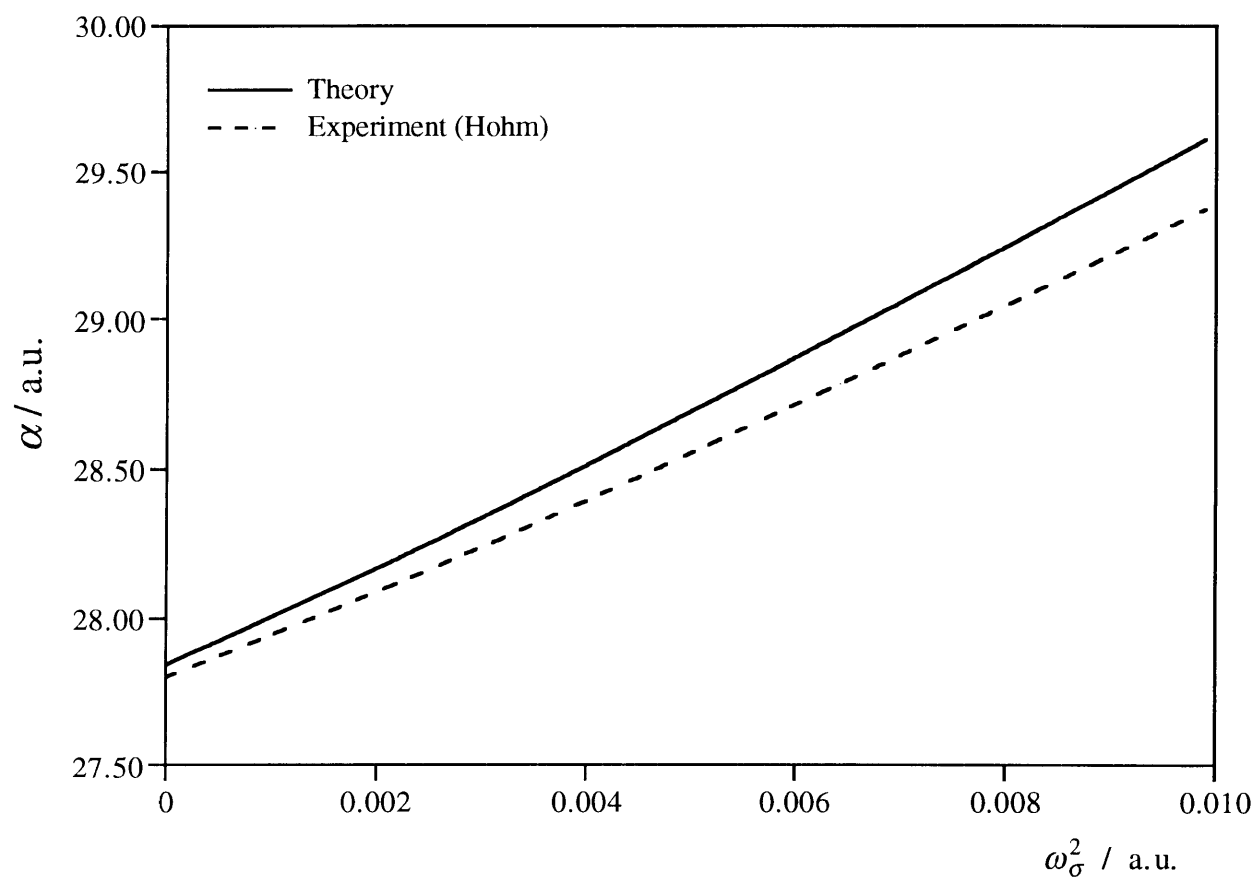
Figure 7.1. Frequency dependence of the mean polarizability for ethene. The solid line is based on pseudo-BD(T) theory and the dashed line is derived from experimental refractivity measurements of Hohm [4].
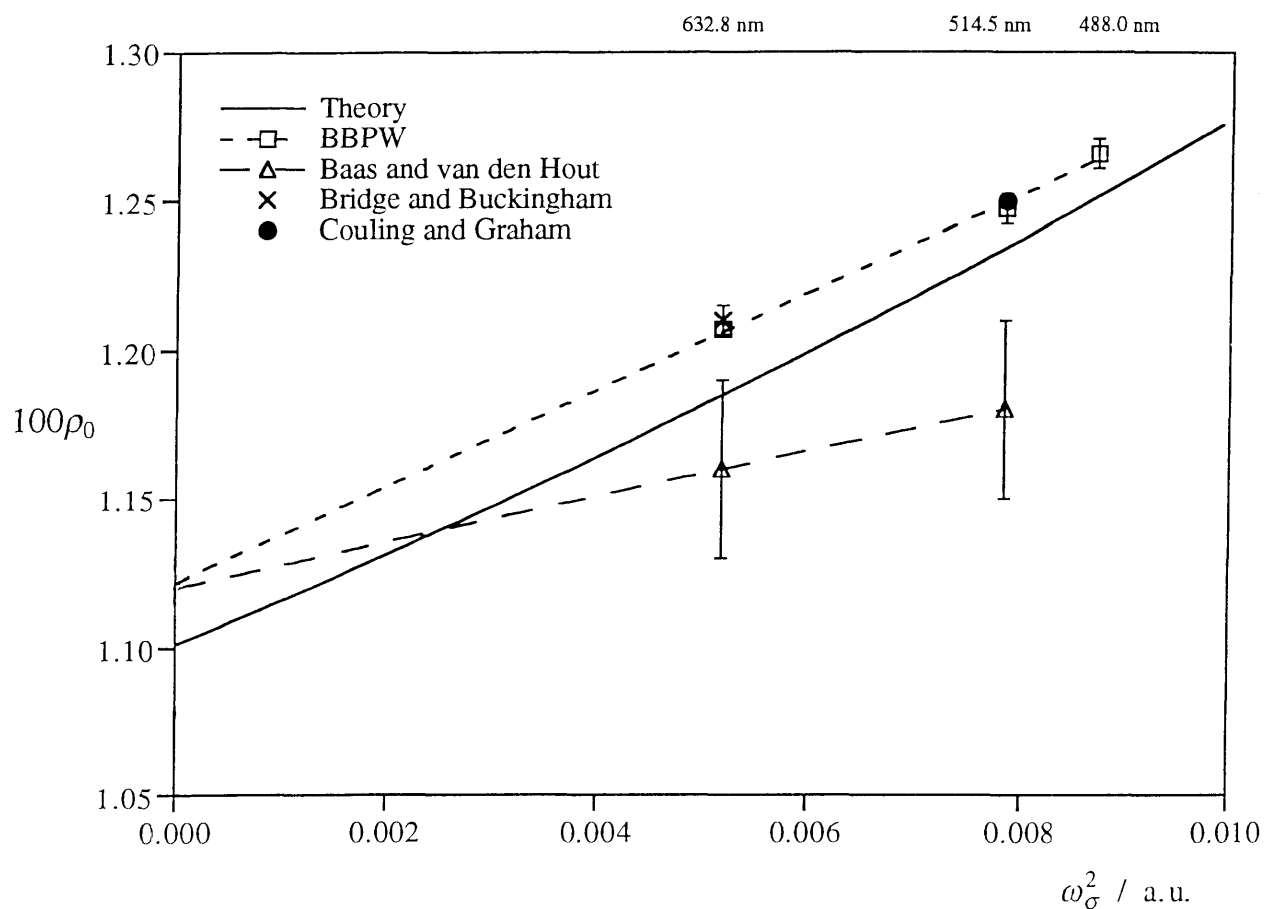
Figure 7.2. Rayleigh depolarization ratios for ethene. The solid line is obtained from pseudo-BD(T) theory with experimental depolarization ratios at dynamic wavelengths from Bogaard, Buckingham, Pierens and White (BBPW) [6], Baas and van den Hout [7], Bridge and Buckingham [8], and Couling and Graham [9].

7.4 Conclusion

The present study of ethene has demonstrated the accuracy attainable via a combination of vibrational corrections with accurate vibrationless properties. Both the moderately sized DZP–ANO3 [$5s3p3d/3s2p$] and DZP–ANO3–H(d) [$5s3p3d/3s2p1d$] basis sets appears to perform extremely well, leading to mean polarizabilities that fall within 0.2% of experiment. Polarizability anisotropies are also well reproduced with theoretical estimates lying within 0.5% of static experimental values deduced from Rayleigh light scattering. Theoretical vibrationally averaged BD(T) estimates of the quadrupole moment for ethene have been found to support the recent rotational Zeeman effect measurements of Majer *et al.* [14].

Properties for the deuterated species CH_2CD_2 and C_2D_4 have been computed and they illustrate the versatility of the theoretical methods utilised in the present thesis. Not only can the computational methods be used to validate the transferability of properties between isotopomers but they may also be used to predict the isotope effects for properties that are difficult to measure, such as the vibrationally induced dipole moment of CH_2D_2. Experimental verification of the electrical properties for CH_2CD_2 and C_2D_4 is currently possible but high accuracy and precision is likely to be necessary to resolve the differences between the properties of C_2H_4, CH_2D_2 and C_2D_4.

Future theoretical work on the frequency dependence of the polarizability and polarizability anisotropy of ethene is necessary. A procedure for calculation of frequency dependent polarizability derivatives would shed light on the frequency dependence of the ZPVC and the polarizability tensor. This may also help to resolve discrepancies between theoretical and experimental depolarization ratios and give insight into the vibrational Raman effect. Experimental measurements of the depolarization ratio, via the methods of Murphy [28] that rigorously exclude the vibrational Raman contribution, would also be of considerable assistance for any future theoretical electrical properties study of ethene.

References

[1]   Watson, H. E., and Ramaswamy, K. L., 1936, *Proc. R. Soc. Lond. A*, **156**, 144.

[2]   Lowery, H., 1931, *Proc. R. Soc. Lond. A*, **133**, 188.

[3]   Landolt-Börnstein, 1962, *Numerical Data and Functional Relationships in Science and Technology*. Vol. VI (Springer-Verlag).

[4]   Hohm, U., 1994, *Molec. Phys.*, **81**, 157.

[5]   Jhanwar, B. L., Meath, W. J., and MacDonald, J. C. F., 1983, *Can. J. Phys.*, **61**, 1027.

[6]   Bogaard, M. P., Buckingham, A. D., Pierens, R. K., and White, A. H., 1978, *J. Chem. Soc. Faraday Trans. I*, **74**, 3008.

[7]   Baas, F., and Van Den Hout, K. D., 1979, *Physica*, **95A**, 597.

[8]   Bridge, N. J., and Buckingham, A. D., 1966, *Proc. R. Soc. Lond. A*, **295**, 334.

[9]   Couling, V. W., and Graham, C., 1996, *Molec. Phys.*, **87**, 779.

[10] Buckingham, A. D., Bogaard, M. P., Dunmur, D. A., Hobbs, C. P., and Orr, B. J., 1970, *Trans. Faraday Soc.*, **66**, 1548.

[11] Tammer, R., and Hüttner, W., 1994, *Molec. Phys.*, **83**, 579.

[12] Chen, Y.-T., and Oka, T., 1988, *J. chem. Phys.*, **88**, 5282.

[13] Hills, G. W., and Jones, W. J., 1975, *J. Chem. Soc. Faraday Trans. II*, **71**, 812.

[14] Majer, W., Lutzmann, P., and Hüttner, W., 1994, *Molec. Phys.*, **83**, 567.

[15] Maroulis, G., 1993, *J. Phys. B: At. Mol. Opt. Phys.*, **26**, 775.

[16] Maroulis, G., 1992, *J. chem. Phys.*, **97**, 4188.

[17] Martí, J., Andrés, J. L., Bertrán, J., and Duran, M., 1993, *Molec. Phys.*, **80**, 625.

[18] Martin, J. M. L., and Taylor, P. R., 1996, *Chem. Phys. Lett.*, **248**, 336.

[19] Herzberg, G., 1954, *Molecular Spectra and Molecular Structure, Vol II. Infrared and Raman Spectra of Polyatomic Molecules* (Van Nostrand).

[20] Nakanaga, T., Kondo, S., and Saëki, S., 1979, *J. chem. Phys.*, **70**, 2471.

[21] Golike, R. C., Mills, I. M., Person, W. B., and Crawford, B., 1956, *J. chem. Phys.*, **25**, 1266.

[22] Jalsovszky, G., and Pulay, P., 1975, *J. molec. Struct.*, **26**, 277.

[23] Bishop, D. M., and Cheung, L. M., 1982, *J. Phys. Chem. Ref. Data*, **11**, 119.

[24] Dagg, I. R., Read, L. A. A., and Smith, W., 1982, *Can. J. Phys.*, **60**, 1431.

[25] Kukolich, S. G., Aldrich, P. D., Read, W. G., and Campbell, E. J., 1983, *J. chem. Phys.*, **79**, 1105.

[26] Hirota, E., Endo, Y., Saito, S., Yoshida, K., and Yamaguchi, I., 1981, *J. molec. Spec.*, **89**, 223.

[27] Lee, T. J., Allen, W. D., and Schaefer III, H. F., 1987, *J. chem. Phys.*, **87**, 7062.

[28] Murphy, W. F., 1977, *J. chem. Phys.*, **67**, 5877.

Ethane

8.1 Introduction

Experimentally, ethane is a well-studied molecule. Over a considerable number of years there have been several determinations of the quadrupole moment [1-4] and only recently have the experimental values been refined [5]. The mean polarizability has received widespread study ranging from the early refractivity measurements by Watson and Ramaswamy [6] to the recent measurements by Hohm [7]. Perhaps the most well-studied but ill-determined electrical property of ethane is the polarizability anisotropy. Measurements of $\Delta\alpha$ from Rayleigh light scattering [8-11], the Cotton-Mouton effect [3] and the microwave Zeeman effect [12-14] have been published but there is still considerable doubt as to which are the most reliable determinations.

Theoretically, high-level *ab initio* calculations of the electrical properties for ethane have been hampered since the basis set size must be carefully considered for electron-correlation calculations. Vibrational averaging studies have not been performed on ethane and larger molecules, presumably due to the difficulty in obtaining the required property derivatives via a straightforward procedure. Least-squares methods could be used for molecules of this size but the large number of displaced geometries and the property calculations at these geometries would prove to be costly. To surmount the problem of least-squares calculation of property derivatives, SCF analytic derivative methods and a finite-difference scheme have been utilised to compute the necessary derivatives. This method allows calculation of first, second and third-order dipole moment, quadrupole moment and polarizability derivatives at the SCF level of theory. Although SCF methods do not yield accurate predictions of electrical properties, they have been shown to give sensible predictions for the zero-point vibrational correction (ZPVC).

The present ZPVCs and pure vibrational polarizabilities, including anharmonic effects, represent the first to be calculated for ethane. As in previous Chapters, accurate BD(T)

vibrationless properties are merged with ZPVCs to provide accurate predictions of the quadrupole moment, polarizability and polarizability anisotropy. It is hoped that comparison of good quality theoretical electrical property predictions with experiment will help to discriminate between different experiments and perhaps indicate the most accurate and reliable experimental results.

8.2 Computational methods

The finite-difference method for computing property derivatives has been outlined in Chapter 3 and was utilised for SCF calculations of DZP–ANO2 and DZP–ANO3 energy and property derivatives. Both the DZP–ANO2 and DZP–ANO3 basis sets have been utilised in previous Chapters on the fluoromethanes (Chapter 6) and ethene (Chapter 7) with exponents and contraction coefficients supplied in Appendix IV. For an N-atomic molecule, the number of analytic second derivative calculations required should be no greater than $2(3N-6)$. Finite-field and finite-field-gradient strengths of 0.001 and 0.0005 au respectively, were used for the SCF, MP2, BD and BD(T) equilibrium electrical property calculations. The MP2/DZP–ANO3 optimized geometry was utilised for these calculations and is supplied in Appendix III. A Fermi resonance tolerance of 200 cm^{-1} was applied to the vibrational calculations. Quartic property derivatives P_4 or cubic property derivatives of the form, P_{ijk}, are not available from the central-differences procedure. Therefore the resulting ZPVCs do not include contributions from these derivatives and should be denoted as ZPVC($-P_4-P_{ijk}$) using the notation of Chapter 7. However, in the interests of clarity, the term ZPVC will be understood to refer to ZPVC($-P_4-P_{ijk}$) for the present Chapter.

8.3 Results and discussion

8.3.1 *Zero-point vibrational corrections and pure vibrational polarizabilities*

Zero-point vibrational corrections (ZPVCs) to the quadrupole moment, polarizability tensor, mean polarizability and polarizability anisotropy are presented in Table 8.1. The relative percentage corrections to the properties of this molecule are quite large and are found to be 10.3, 5.6 and 5.7% for Θ_{zz}, α and $\Delta\alpha$ respectively with the DZP–ANO3 basis set. Quadrupole moment corrections are positive in sign and act to decrease the magnitude of Θ_{zz}. The smaller DZP–ANO2 basis set also gives corrections of similar magnitude for the mean polarizability but yields a 7.9% correction to the quadrupole moment and a larger 7.0% contribution to $\Delta\alpha$. Interestingly, the relative corrections to tensor components α_{xx} and α_{zz} obtained with the DZP–ANO3 basis set are virtually the same. The corrections in Table 8.1

represent the largest relative corrections to the mean polarizability of any molecule studied to date, primarily due to the presence of many C–H bonds that effectively increase the overall molecular size. Longer-chain alkanes should exhibit even larger ZPVCs to the mean polarizability and it may be possible to develop an approximate extrapolation procedure for computing the ZPVCs to the polarizability of C_8H_{18} or larger alkanes, based on the ZPVCs to α for CH_4, C_2H_6 and C_3H_8. The resulting model would be similar in approach to the bond polarizability models of Applequist *et al.* [15] and Miller *et al.* [16].

Table 8.1.

SCF DZP–ANO2 and DZP–ANO3 vibrationless properties and zero-point vibrational corrections (ZPVCs) (in au) to the electrical properties of ethane.[a]

Property	DZP–ANO2		DZP–ANO3	
	P_e	ZPVC	P_e	ZPVC
Θ_{zz}	−0.5856	0.04589	−0.5751	0.05892
α_{xx}	26.096	1.4287	26.000	1.4470
α_{zz}	29.553	1.6700	29.355	1.6387
α	27.249	1.5091	27.118	1.5109
$\Delta\alpha$	3.457	0.2413	3.355	0.1916

[a] Quadrupole moment corrections were derived from quadrupole moments relative to the centre of mass.

The pure vibrational polarizabilities, presented in Table 8.2, are in reasonable agreement with experiment, given the restriction of this study to the SCF level of theory. Electron correlation is expected to decrease the magnitude of theoretical predictions thereby bringing the current results closer to experiment. Changing the v_9 vibrational fundamental intensity from 6.10(4) [17, 18] to 7.9(4) km mol^{-1} [19] tends to increase the perpendicular α_{xx}^v component, leading to improved agreement with theory for the pure vibrational polarizability anisotropy and mean polarizability.

Table 8.2.

SCF DZP–ANO2 and DZP–ANO3 ground state pure vibrational polarizabilities (in au) for ethane.[a]

	DZP–ANO2	DZP–ANO3	Experiment
α_{xx}^v	0.4723	0.4520	0.392[a], 0.423[b]
α_{zz}^v	0.2243	0.2216	0.210 , 0.210
α^v	0.3896	0.3752	0.331(17), 0.352(18)
$\Delta\alpha^v$	−0.2480	−0.2304	−0.182(9), −0.213(11)

[a] Derived from experimental infrared intensities [17, 18].

[b] Derived from experimental infrared intensities from (a) but with a more recent measurement for the v_9 intensity [19].

8.3.2 *Comparison with experiment*

Vibrationally averaged theoretical predictions of the electrical properties of ethane are compared with experimental results in Table 8.3. Addition of the ZPVC to the vibrationless BD(T) quadrupole moment of −0.5804 au leads to a value of −0.5215 au in fine agreement with both the field-gradient-induced birefringence (FGIB) measurement of Watson [5] and also the Cotton-Mouton results of −0.56(6) and −0.51(21) au from Coonan [20] and Kling *et al.* [3], respectively. The theoretical predictions lie within the range of uncertainties for the above experiments and this is a most gratifying result. Another FGIB measurement of −0.74(3) au for the quadrupole moment has been published [1] but appears to be too large in comparison to other measurements. Dagg *et al.* [4] have derived quadrupole moments in the range from −0.50 to an upper-limit of −0.95 au from collision-induced absorption measurements. Present *ab initio* and accurate FGIB experiments obviously support the smaller values of Θ_{zz}.

Predictions of the static mean polarizability from BD(T) theory also appear to be quite accurate and are exceptionally close to an extrapolated estimate from Hohm [21] and the DOSD number from Jhanwar *et al.* [22]. Other mean polarizabilities, derived from quadratic extrapolations of refractivity data, yield 29.673(3) au [6], 30.056(6) au [23, 24], and 29.768(5) au [25]. The doubles contribution at the MP2 level of theory leads to an overestimate of α (with respect to more accurate BD(T) values), inclusion of quadruple and higher substitutions for BD decreases the mean polarizability while the perturbative triple excitations for BD(T) tend to shift the value of α back towards experiment. The polarizability anisotropy from BD(T) theory is in exact agreement with the extrapolated estimate from Rayleigh light scattering [9]. An improvement in basis set quality is expected to yield a larger value of the anisotropy thereby giving better agreement with the static $\Delta\alpha$ of Bogaard *et al.* [8].

Presenting only static estimates of $\Delta\alpha$ would ignore the larger number of experimental investigations at laser wavelengths for this property. In order to suitably compare theory with experiment, pseudo-BD(T) mean polarizabilities and polarizability anisotropies have been calculated at six laser wavelengths and plotted with experimental results in Figures 8.1 and 8.2. The theoretical pseudo-BD(T)/DZP–ANO3 frequency dependence of the mean polarizability matches, almost exactly, the frequency dependence derived from measurements by Hohm [21]. Experimental polarizability anisotropies presented in Figure 8.2 have all been calculated from Rayleigh depolarization ratios and a consistent set of interpolated dynamic mean polarizabilities from Hohm [21].

Table 8.3.

Vibrationally averaged quadrupole moments, polarizabilities and polarizability anisotropies (in au) of ethane.[a]

Property	Level of Theory				Experiment
	SCF	MP2	BD	BD(T)	
Θ_{zz}	−0.5146	−0.5560	−0.5173	−0.5215	−0.50(3)[b], −0.51(21)[c]
α_{xx}	27.696	28.481	28.105	28.334	
α_{zz}	31.211	32.566	31.864	32.216	
α	28.868	29.843	29.358	29.628	29.561(8)[d], 29.613[e]
$\Delta\alpha$	3.514	4.085	3.759	3.882	4.17(12)[f], 3.88(13)[g]

[a] SCF/DZP–ANO3 vibrational corrections have been applied to property calculations at the respective theoretical MP2/DZP–ANO3 geometry using the DZP–ANO3 basis set for the vibrationless properties. Quadrupole moments refer to centre of mass coordinates.

[b] Electric field-gradient-induced birefringence measurement [5].

[c] Cotton-Mouton effect measurement [3].

[d] Static estimate from a quadratic extrapolation of polarizability data (five wavelengths between 633 and 325 nm) [21].

[e] DOSD static estimate [22].

[f] Static estimate from an extrapolation to zero frequency of $\Delta\alpha(\omega_\sigma)$, obtained from Rayleigh depolarization ratios [8] combined with interpolated dynamic mean polarizabilities [21].

[g] Static estimate from two-point extrapolation of $\Delta\alpha(\omega_\sigma)$ from Rayleigh depolarization ratios [9] combined with interpolated dynamic mean polarizabilities [21].
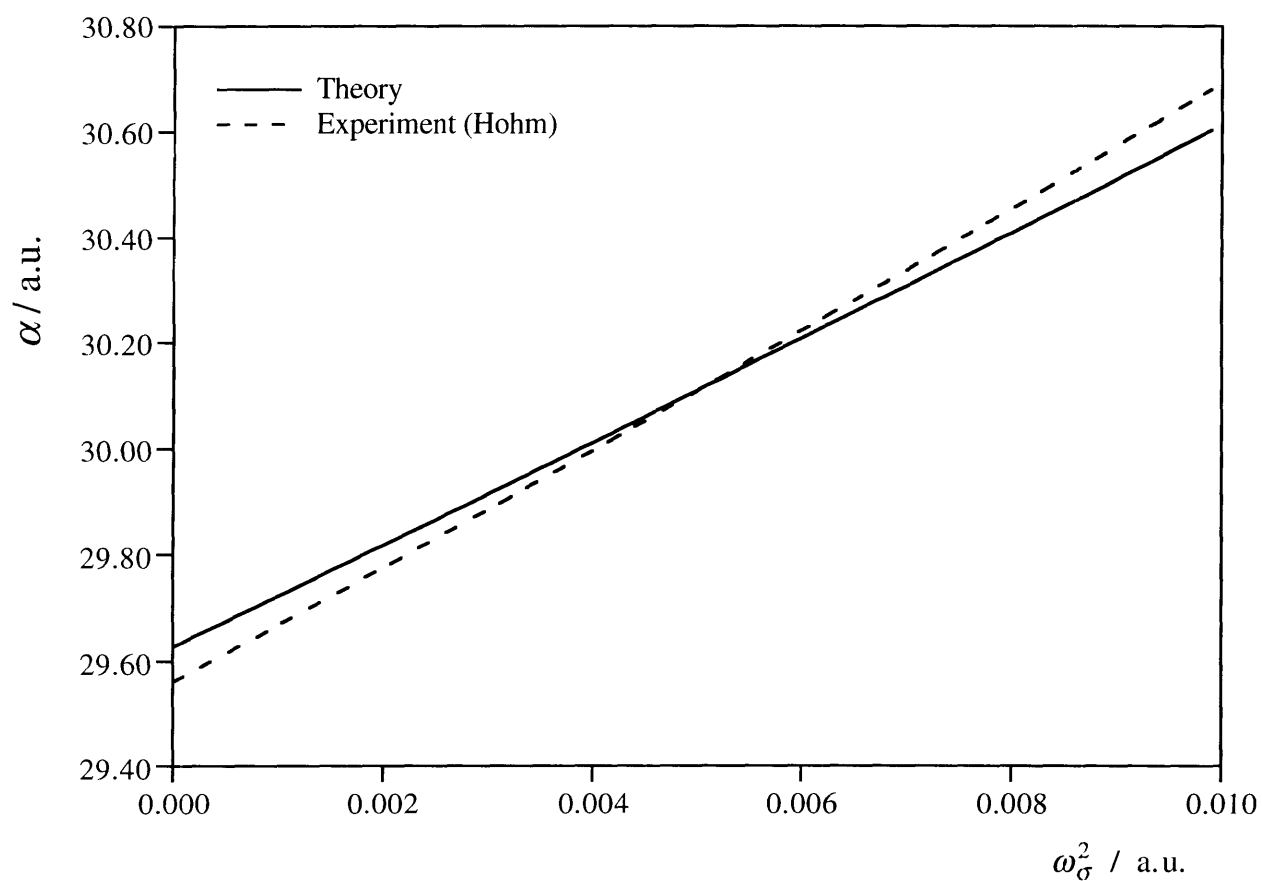
Figure 8.1. Frequency dependence of the mean polarizability for ethane. The solid line is based on pseudo-BD(T) theory and the dashed line is derived from experimental refractivity measurements of Hohm [21].
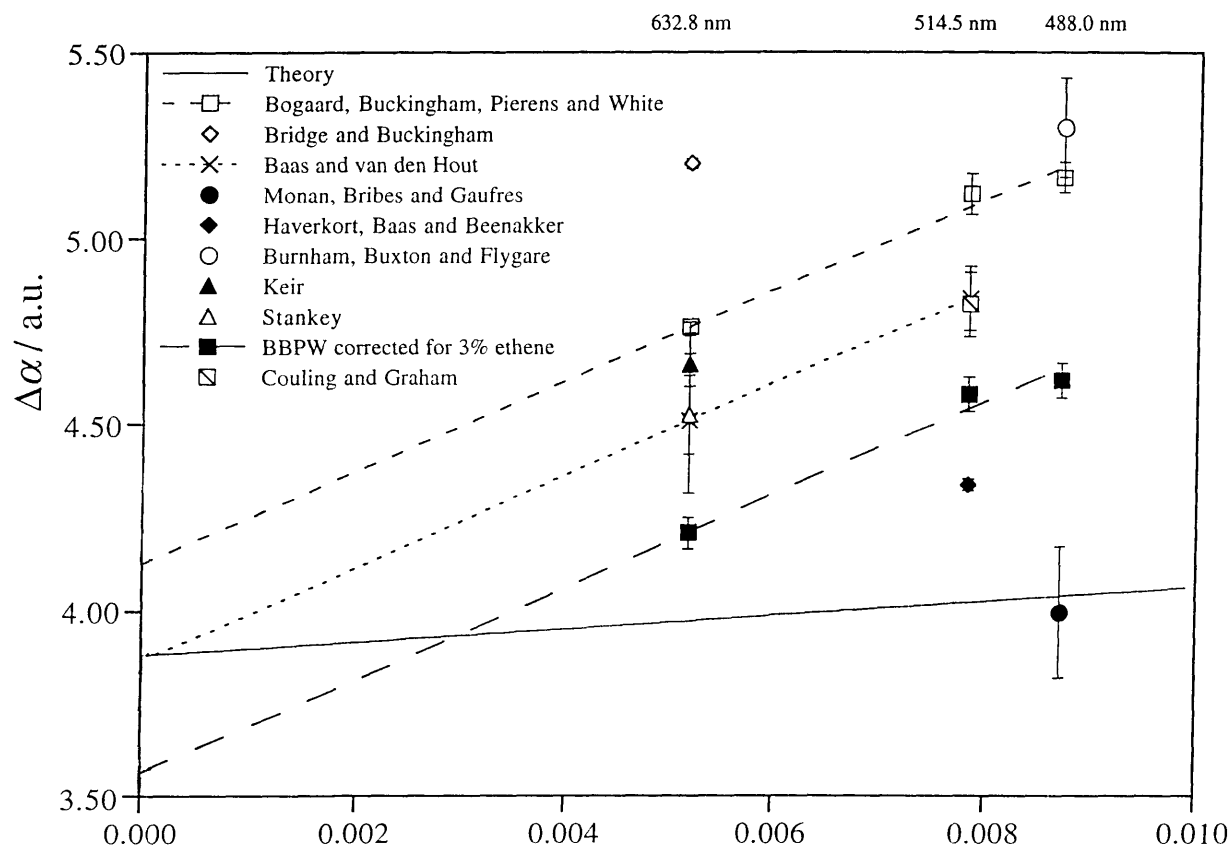
Figure 8.2. Frequency dependence for the polarizability anisotropy of ethane. The solid line is obtained from pseudo-BD(T) theory with experimental polarizability anisotropies at dynamic wavelengths derived using Rayleigh depolarization ratios from various sources ([8-11, 26-30]) and a consistent set of interpolated mean polarizabilities from Hohm [21].

Agreement with the vast number of experimental measurements for the polarizability anisotropy appears to be poor, although the vibrational Raman effect clearly influences the derived $\Delta\alpha$ from Rayleigh light scattering. An estimate of $\Delta\alpha$ from Monan *et al.* [11] at 488.0 nm that excludes the vibrational Raman contribution to the Rayleigh depolarization ratio, lies very close to the theoretical pseudo-BD(T) $\Delta\alpha$ curve. Furthermore, the extrapolated static estimate from Baas and van den Hout [9] agrees extremely well with theory, giving confidence in the accuracy of the present BD(T) static predictions. More recent results from Keir [27], Stankey [28], and Couling and Graham [26] support the Baas and van den Hout predictions. Corrected values of the ethane measurements of Bogaard, Buckingham, Pierens and White [8] assuming an ethane sample of 3% ethene reported in Coonan [20], lead to a frequency dependence that has identical slope but smaller static $\Delta\alpha$ (intercept) when compared to the Baas and van den Hout [9] results. An accurate static experimental value for the polarizability anisotropy has been calculated utilising a combination of Cotton-Mouton effect data, Rayleigh light scattering depolarization ratios and electric-field-induced birefringence [20]. The experimental value of 4.2(3) au [20], when corrected for a pure vibrational contribution of $-0.213(11)$ au from Table 8.2, leads to 4.0(3) au which is quite accurate but with a large uncertainty.

To test the effect of internal rotation on the electrical properties for ethane, the quadrupole moment and polarizability tensor, at the BD(T) level of theory, have been calculated with an eclipsed MP2/DZP–ANO3 optimized geometry. Differences between the electrical properties at staggered and eclipsed conformations ($P_{staggered} - P_{eclipsed}$), with the exception of the polarizability anisotropy, are relatively small (Θ_{zz}, α, $\Delta\alpha$) = (-0.00014, 0.09829, -0.33678 au). The barrier height for the internal rotation in ethane has been measured to be 1013.29(24) cm^{-1} [12, 13](12.1216(28) kJ mol^{-1}) and therefore at the temperatures that many of the measurements were performed (300 K) ($RT \approx 2.5$ kJ mol^{-1}), it can be reasonably assumed that the experimental results correspond to ground vibrational state values (staggered conformation).

8.3.3 Isotope effects : properties of CH_3CD_3 and C_2D_6

Zero-point vibrational corrections (ZPVCs) to the electrical properties of the isotopomers C_2H_6, CH_3CD_3 and C_2D_6 are presented in Table 8.4. Quadrupole moment corrections show a regular decrease with deuterium isotopic substitution, as observed for ethene, and are exceptionally small. Differences between the quadrupole moments for the these isotopomers are approximately of the order of the experimental uncertainties and therefore

extremely accurate measurements would be required to determine the isotopic difference. Deuterium isotope effects for the mean polarizability may be measurable via accurate refractivity measurements such as those carried out by Hohm [7]. Curiously, the polarizability anisotropy is approximately independent of isotopic substitution, thus suggesting that the polarizability tensor components are affected by similar amounts with deuterium substitution. Experimental molecular Zeeman effect measurements on CH_3CD_3 [12, 13] should therefore be capable of providing reliable estimates of $\Delta\alpha$ for C_2H_6. Ozier and Meerts' value of 4.53(18) au for $\Delta\alpha$ [12, 13] is approximately 17% larger than other static estimates. A vibrationally induced SCF/DZP–ANO3 dipole moment of −0.0051796 au is reasonably close to the experimental values of −0.0042733(2) au [12, 13] from the second-order Stark effect and −0.00424(4) au from microwave spectroscopy [31], given the small size of the quantities and the SCF level of approximation for the vibrational correction. Higher levels of theory, such as MP2, are probably necessary to obtain improved accuracy for the vibrationally induced dipole moment.

Table 8.4.

SCF DZP–ANO3 zero-point vibrational corrections (in au) to the electrical properties of ethane, 1,1,1-trideuteroethane and perdeuteroethane.[a]

| Property | ZPVCs | | |
	CH_3CH_3	CH_3CD_3	CD_3CD_3
Θ_{zz}	0.05892	0.04492	0.03954
α_{xx}	1.4470	1.2475	1.0658
α_{zz}	1.6387	1.4563	1.2661
α	1.5109	1.3171	1.1326
$\Delta\alpha$	0.1916	0.2088	0.2003

[a] Quadrupole moment corrections refer to the centre of mass coordinates.

Pure vibrational polarizabilities for C_2H_6 and C_2D_6 are compared in Table 8.5 with vibrational polarizabilities derived from experimental infrared intensity measurements. Ethane is one such molecule for which the intensities of both parent and perdeuterated isotopomers have been determined [17, 18]. If the experimental data for C_2H_6 of Nyquist *et al.* [18] are supplemented with a v_9 infrared band intensity from Varanasi *et al.* [19], the isotopic effect ($C_2H_6 - C_2D_6$) for the polarizabilities agree well with theoretical SCF/DZP–ANO3 estimates (see Table 8.2).

Table 8.5.

SCF DZP–ANO3 ground state pure vibrational polarizabilities

(in au) for ethane and perdeuteroethane.

Isotopomer		Theory	Experiment
CH_3CH_3	α_{xx}^v	0.4520	0.423[b]
	α_{zz}^v	0.2216	0.210
	α^v	0.3752	0.352(18)
	$\Delta\alpha^v$	−0.2304	−0.213(11)
CD_3CD_3	α_{xx}^v	0.4414	0.408[a]
	α_{zz}^v	0.2182	0.217
	α^v	0.3670	0.344(20)
	$\Delta\alpha^v$	−0.2232	−0.190(11)

[a] Derived from experimental infrared intensities [17, 18].

[b] Derived from experimental infrared intensities from (a) but with a more recent measurement for the v_9 intensity [19].

8.3.4 *Temperature dependence*

Temperature dependent measurements of the polarizability have been reported by Kerl and Haüsler [32] and are reproduced in [33]. Unfortunately, the original measurements suffer from an artificial temperature dependence thus leading to an apparent temperature dependence that is much too large. As an indication of the effect of temperature on the electrical properties, thermal corrections for 300 K, $\langle P \rangle^{300 \text{ K}} - \langle P \rangle_0$, have been calculated using the approximate method described in Chapter 2 (see equation (2.71)). For the quadrupole moment, the SCF/DZP–ANO3 thermal correction has been calculated to be 0.0001 au. For the mean polarizability and polarizability anisotropy respectively, values of 0.0009 and 0.0246 au have been obtained. Although the magnitude of the thermal correction, compared to other properties, is relatively large for $\Delta \alpha$ (12.8% of the ZPVC and 0.67% of the vibrationless property), considering the accuracy of the Rayleigh light scattering results in Table 8.3, the inclusion of the thermal correction within the *ab initio* prediction is probably not warranted. The thermal correction is approximately 5 times smaller than the uncertainties for the two experimental static $\Delta \alpha$ estimates of 4.17(12) [8] and 3.88(13) au [9], and therefore would not play a significant role in discriminating between the two experiments.

8.4 Conclusion

The present study of ethane illustrates the utility of the present theoretical method for calculation of ZPVCs and pure vibrational polarizabilities. Not only may ethane be treated but the electrical properties for isotopomers can also be investigated. The SCF vibrational corrections appear to be largely successful in accounting for the difference between vibrationless theoretical predictions and experimental measurements. In many instances, and especially for studies of larger molecules, the central difference derivatives method, in conjunction with SCF or DFT methods, is likely to provide a cost effective route to calculation of electrical property derivatives as compared with least-squares fitting methods.

Recent quadrupole moment measurements from the FGIB method [5] appear to be exceptionally accurate and the measurements of Hohm [7] have been identified as currently the most reliable values for the mean polarizability.

Through study of the polarizability anisotropy for ethane, it has become apparent that there is a wide variation in experimental estimates and this is primarily due to the vibrational Raman contribution to observed depolarization ratios. Extrapolated Rayleigh light scattering measurements of Baas and van den Hout [9], Keir [27], Stankey [28], Couling and Graham [26]

and Monan *et al.* [11] are possibly the most accurate for this molecule. Future theoretical work should be focused on examining the role of the vibrational Raman contribution to the Rayleigh depolarization ratio as it is undoubtedly clear that, for molecules with small depolarization ratios (and polarizability anisotropies), dynamic theoretical and experimental depolarization ratios do not refer to the same quantity, and hence are not strictly comparable. It is hoped that further experimental and theoretical work will help to refine values of the electrical properties.

References

[1]   Buckingham, A. D., Graham, C., and Williams, J. H., 1983, *Molec. Phys.*, **49**, 703.

[2]   Buckingham, A. D., Disch, R. L., and Dunmur, D. A., 1968, *J. Am. Chem. Soc.*, **90**, 3104.

[3]   Kling, H., Geschka, H., and Hüttner, W., 1983, *Chem. Phys. Lett.*, **96**, 631.

[4]   Dagg, I. R., Smith, W., and Read, L. A. A., 1982, *Can. J. Phys.*, **60**, 16.

[5]   Watson, J. N., 1995, PhD Thesis, University of New England, Armidale NSW, Australia.

[6]   Watson, H. E., and Ramaswamy, K. L., 1936, *Proc. R. Soc. Lond. A*, **156**, 144.

[7]   Hohm, U., 1994, *Chem. Phys.*, **179**, 533.

[8]   Bogaard, M. P., Buckingham, A. D., Pierens, R. K., and White, A. H., 1978, *J. Chem. Soc. Faraday Trans. I*, **74**, 3008.

[9]   Baas, F., and Van Den Hout, K. D., 1979, *Physica*, **95A**, 597.

[10] Bridge, N. J., and Buckingham, A. D., 1966, *Proc. R. Soc. Lond. A*, **295**, 334.

[11] Monan, M., Bribes, J.-L., and Gaufrès, R., 1982, *J. Raman. Spectrosc.*, **12**, 190.

[12] Ozier, I., and Meerts, W. L., 1984, *Can. J. Phys.*, **62**, 1844.

[13] Ozier, I., and Meerts, W. L., 1985, *Can. J. Phys.*, **63**, 1375.

[14] Hüttner, W., Häussler, H., and Majer, W., 1984, *Chem. Phys. Lett.*, **109**, 359.

[15] Applequist, J., Carl, J. R., and Fung, K.-K., 1972, *J. Am. Chem. Soc.*, **94**, 2952.

[16] Miller, K. J., 1990, *J. Am. Chem. Soc.*, **112**, 8543.

[17] Bishop, D. M., and Cheung, L. M., 1982, *J. Phys. Chem. Ref. Data*, **11**, 119.

[18] Nyquist, I. M., Mills, I. M., Person, W. B., and Crawford, B., 1957, *J. chem. Phys.*, **26**, 552.

[19] Varanasi, P., Cess, R. D., and Bangaru, B. R. P., 1974, *J. Quant. Spectrosc. Radiat. Transfer*, **14**, 1107.

[20] Coonan, M. H., 1995, PhD Thesis, University of New England, Armidale NSW, Australia.

[21]   Hohm, U., 1994, *Molec. Phys.*, **81**, 157.

[22]   Jhanwar, B. L., Meath, W. J., and MacDonald, J. C. F., 1981, *Can. J. Phys.*, **59**, 185.

[23]   Friberg, S., 1931, *Z.Physik*, **73**, 216.

[24]   Landolt-Börnstein, 1962, *Numerical Data and Functional Relationships in Science and Technology.* Vol. VI (Springer-Verlag).

[25]   Lowery, H., 1931, *Proc. R. Soc. Lond. A*, **133**, 188.

[26]   Couling, V. W., and Graham, C., 1994, *Molec. Phys.*, **82**, 235.

[27]   Keir, R. I., 1995, PhD Thesis, University of New England, Armidale NSW, Australia.

[28]   Stankey, R., 1991, M.Sc. Thesis, University of New England, Armidale, NSW, Australia.

[29]   Burnham, A. K., Buxton, L. W., and Flygare, W. H., 1977, *J. chem. Phys.*, **67**, 4990.

[30]   Haverkort, J. E. M., Baas, F., and Beenakker, J. J. M., 1983, *Chem. Phys.*, **79**, 105.

[31]   Hirota, E., and Matsumara, C., 1971, *J. chem. Phys.*, **55**, 981.

[32]   Kerl, K., and Häusler, H., 1984, *Ber. Bunsenges. Phys. Chem.*, **88**, 992.

[33]   Hohm, U., and Kerl, K., 1986, *Molec. Phys.*, **58**, 541.

Conclusions

Through the present investigations into vibrational and rotational corrections to molecular properties, the requirements for obtaining accurate *ab initio* theoretical predictions have been established. It has been shown that accurate vibrationless properties are necessary to obtain quantitative agreement with experiment, before any vibrational and rotational corrections are applied. Basis set quality is an important part of realising high quality electrical property estimates; for the smaller molecules, such as SiH_4, PH_3, H_2S, HCl, C_2H_4 and C_2H_2, large basis sets have been applied and present results for these molecules are especially good. For larger molecules, compromises in basis set quality must be made, which was the primary reason for using the DZP–ANO type of basis sets for the fluoromethanes and C_2H_6.

Accurate geometries, derived from either experiment or high level *ab initio* calculations, are also important for obtaining good quality properties. In particular, the dipole moments appear to be quite susceptible to errors in underlying geometries because the vibrational corrections are often small in terms of a percentage correction to the uncorrected property. Other properties, for which the relative vibrational correction is substantial, are not as susceptible to the problem of inaccurate geometries.

Adequate treatment of electron correlation is also a consideration for *ab initio* theoretical predictions. The Brueckner doubles (BD) method and the BD(T) counterpart have been used extensively in the present thesis. These sophisticated and accurate methods for treating electron correlation have been used to provide the first reported BD(T) electrical property estimates for many of the studied molecules. Results from MP4 or CCSD(T) calculations, for the same basis sets and molecular geometries, are expected to be comparable to those obtained in the present thesis. Often the highest quality theoretical method utilised, whether it is BD(T), MP4, CCSD(T) or QCISD(T), is dictated by the

availability of particular *ab initio* quantum chemical programs. Some care must be used with methods that are theoretically incomplete such as MP3, MP4-SDQ, BD, QCISD or CCSD. It has been found that for the molecules studied in the present thesis, the perturbative triples (T) correction is almost essential for obtaining accurate and reliable electrical properties.

In many cases, the current investigations represent the first vibrational and rotational studies undertaken for the electrical properties of the selected molecules. The most useful contribution for obtaining quantitative agreement with experiment is the zero-point vibrational correction (ZPVC). Generally, it has been found that for dipole moments, the corrections are relatively small, usually < 1% of the uncorrected property. For quadrupole moments, the ZPVCs are typically smaller than 2% of the uncorrected property. Polarizabilities are found to have larger relative corrections closer to 5% of the uncorrected property. In cases where the uncorrected polarizability anisotropy is small, the relative zero-point vibrational correction can be particularly large; this was effectively demonstrated for H_2S where a 49% correction to $\Delta\alpha$ at the MP2 level was computed. However, for the majority of molecules, a relative percentage correction in the range 5-10% is expected for the polarizability anisotropy. Differences between SCF and MP2 vibrational corrections are usually small; in many cases the SCF corrections, in conjunction with accurate vibrationless properties, will be sufficient for obtaining quantitative agreement with experiment and this is especially useful for studies on large molecules.

Deuterium isotope effects offer an interesting avenue for *ab initio* theory. Perhaps the most successful demonstration of the present theoretical methods relates to the mean polarizabilities of H_2S and HCl where accurate measurements for the deuterated isotopomers exist. However, the theoretical calculation of isotope effects also plays a useful role in verifying the accuracy of experimental measurements on isotopically substituted molecules. One such example occurs for the quadrupole moment determination for CH_2CD_2 from molecular Zeeman effect measurements [1], where the present *ab initio* calculations have established the differences between zero-point vibrational effects and the transferability of the measured quadrupole moment tensor for C_2H_4 and CH_2CD_2.

Thermal corrections are expected to be less important in theoretical predictions for obtaining quantitative with experiment. Most electrical property experiments are carried out at temperatures close to 300 K, so for the majority of cases only the ground vibrational state is significantly populated thus leading to small thermal corrections of magnitude approximately 1% of the zero-point vibrational correction. For instances where an

experimental temperature dependence of the property is available, such as those measured for the polarizability by Hohm *et al.* [2], the theory outlined in the present thesis will allow a theoretical investigation of the temperature dependence for the property.

Pure vibrational polarizabilities have been presented and compared with experimental estimates derived from infrared intensity data. It is anticipated that *ab initio* theoretical methods will be of considerable assistance in the determination of such properties as a complete set of experimental dipole transition elements, required for the experimental pure vibrational polarizabilities, is often difficult to obtain for large molecules. Pure vibrational polarizabilities are helpful in the analysis of data from Kerr effect and dielectric constant experiments. However, they are not as useful as the ZPVC for obtaining quantitative agreement with experiment. Vibrational contributions to higher-order electrical response properties [3-8], such as the pure vibrational first and second-hyperpolarizabilities (β^v and γ^v respectively), are likely to be more important for the analysis of experimental results. Much of the theory for calculation of vibrational contributions has been presented in the thesis. Hyperpolarizability and dipole-polarizability derivatives are required for β^v and γ^v and calculation of these quantities, especially at MP2 or higher levels of theory, is expected to require considerable computational effort. Nevertheless, there is considerable scope in this area for *ab initio* theory and further study may also lead to closer collaborations between theoreticians and experimentalists.

Future theoretical work in the area of vibrational and rotational contributions to molecular properties should be focused on a number of areas. One area would involve the development of a finite-field approach for calculation of polarizability derivatives and hyperpolarizability derivatives. This would involve finite-field calculation of the polarizability and the hyperpolarizability for given molecular geometry, followed by least-squares fitting of the properties to obtain (hyper)polarizability derivatives. Analytic MP2 second derivatives for the polarizability utilise a large amount of disk storage for molecules without symmetry, so a numerical method may offer a way to save disk usage. However, there is a potential disadvantage with this approach, namely the possibility of numerical inaccuracy arising from both the finite-field polarizability and the least-squares derivatives calculations. Nevertheless, a finite-field method would probably be useful for other higher-level theoretical methods, such as BD(T), where analytic second derivatives and analytic polarizabilities are not yet currently available.

A relatively straightforward addition to the current least-squares method would involve the calculation of SCF frequency dependent polarizability derivatives. This would

lead to computation of dynamic polarizabilities and polarizability anisotropies for particular rotational-vibrational states. It is hoped that this would lead to a better understanding of the frequency dependence of both α and $\Delta\alpha$, since the frequency dependent behaviour of the ZPVC and other vibrational corrections is presently unknown. Once the role of frequency dependent vibrational corrections to $\Delta\alpha$ has been established, a further step would involve an exploration of the vibrational Raman contribution to the Rayleigh depolarization ratio, ρ_0. Such an investigation is likely to be of considerable assistance to both theoreticians and experimentalists, since a routine theoretical method for calculation of vibrational Raman contributions would enable a better comparison between theoretical and experimental Rayleigh light scattering data. As a consequence of the present studies on the fluoromethanes, ethane and the second-row hydrides, it appears that a Rayleigh light scattering apparatus (equipped with an optical filter) does not fully exclude the vibrational Raman contribution from the observed depolarization ratio. The method first proposed by Murphy [9] rigorously excludes the vibrational Raman contribution and utilises a combination of rotational Raman spectroscopy and Rayleigh depolarization ratios. Further experimental measurements via this procedure would help to pinpoint the magnitude of the vibrational Raman contribution to the observed depolarization ratio.

Another direction for further work is the development of a hybrid theoretical method thus allowing calculation of property derivatives at a non-stationary point on the potential energy surface. For example, an MP2 anharmonic force field could be combined with SCF property derivatives calculated at a BD(T) optimized reference geometry to compute rotational-vibrational property corrections. Such a method would lead to considerable savings in computational effort but a suitable procedure for projecting out the gradient terms from the higher-order energy derivatives would need to be developed. Some progress in this area has been made for potential energy surfaces and fundamental frequencies [10, 11] but other property surfaces remain largely unexplored.

Naturally, the theoretical methods described in this thesis for computing rotational and vibrational contributions to molecular properties are entirely general. Therefore, other properties such as higher multipole moments, magnetizabilities, electric field-gradients at the nuclei and hyperpolarizabilities could be treated in a straightforward manner. The least-squares approach is well suited to other molecular properties as only the property at a given molecular geometry is required and no further development of analytic derivative methods is necessary. The method is also not limited to any one particular *ab initio* quantum chemical

program so ANHARPS [12] could be interfaced to other codes such as GAUSSIAN [13] or GAMESS [14], rather than relying purely on CADPAC [15].

Only with successful interaction between theory and experiment can many of the problems outlined in the thesis be tackled. There are numerous projects that could benefit from enhanced theoretical and experimental collaboration, two of which are the vibrational Raman contribution to Rayleigh light scattering depolarization ratios and the temperature dependence of electrical properties. It is hoped that the present thesis will stimulate further work in this profitable area and in particular, assist the cooperative process between theory and experiment.

References

[1] Majer, W., Lutzmann, P., and Hüttner, W., 1994, *Molec. Phys.*, **83**, 567.

[2] Hohm, U., and Kerl, K., 1986, *Molec. Phys.*, **58**, 541.

[3] Kirtman, B., and Bishop, D. M., 1990, *Chem. Phys. Lett.*, **175**, 601.

[4] Martí, J., and Bishop, D. M., 1993, *J. chem. Phys.*, **99**, 3860.

[5] Bishop, D. M., and Kirtman, B., 1992, *J. chem. Phys.*, **97**, 5255.

[6] Bishop, D. M., and Kirtman, B., 1991, *J. chem. Phys.*, **95**, 2646.

[7] Bishop, D. M., Kirtman, B., Kurtz, H. A., and Rice, J. E., 1993, *J. chem. Phys.*, **98**, 8024.

[8] Bishop, D. M., 1994, *Adv. Quantum Chem.*, **25**, 1.

[9] Murphy, W. F., 1977, *J. chem. Phys.*, **67**, 5877.

[10] Allen, W. D., and Császár, A. G., 1993, *J. chem. Phys.*, **98**, 2983.

[11] Green, W. H., Jayatilaka, D., Willetts, A., Amos, R. D., and Handy, N. C., 1990, *J. chem. Phys.*, **93**, 4965.

[12] Russell, A. J., 1995, Anharmonic Property Surface Package, ANHARPS 2.0.

[13] Frisch, M. J., Trucks, G. W., Schlegel, H. B., Gill, P. M. W., Johnson, B. G., Robb, M. A., Cheeseman, J. R., Keith, T., Petersson, G. A., Montgomery, J. A., Raghavachari, K., Al-Laham, M. A., Zakrzewski, V. G., Ortiz, J. V., Foresman, J. B., Peng, C. Y., Ayala, P. Y., Chen, W., Wong, M. W., Andres, J. L., Replogle, E. S., Gomperts, R., Martin, R. L., Fox, D. J., Binkley, J. S., Defrees, D. J., Baker, J., Stewart, J. P., Head-Gordon, M., Gonzalez, C., and Pople, J. A., 1995, Gaussian 94.

[14]   Schmidt, M. W., Baldridge, K. K., Boatz, J. A., Elbert, S. T., Gordon, M. S., Jensen, J. H., Koseki, S., Matsunaga, N., Nguyen, K. A., Su, S. J., Windus, T. L., Dupuis, M., and Montgomery, J. A., 1993, *J. Comp. Chem.*, **14**, 1347.

[15]   Amos, R. D., Alberts, I. L., Andrews, J. S., Colwell, S. M., Handy, N. C., Jayatilaka, D., Knowles, P. J., Kobayashi, R., Noga, N., Laidig, K. E., Maslen, P. E., Murray, C. W., Rice, J. E., Sanz, J. E., Simandiras, E. D., Stone, A. J., and Su, M.-D., 1994, CADPAC: The Cambridge Analytic Derivatives Package, issue 5.2.

Appendices

Appendix I. Conversion factors

For converting between Hartree atomic units and SI units.

Energy E	Hartree	$1\ E_h$	$=$	$4.3597482 \times 10^{-18}$ J
Length	Bohr	$1\ a_0$	$=$	$0.529177249 \times 10^{-10}$ m
Dipole moment μ		$1\ ea_0$	$=$	8.478358×10^{-30} C m
Quadrupole moment Θ		$1\ ea_0^2$	$=$	4.486554×10^{-40} C m²
Dipole-polarizability α		$1\ e^2 a_0^2 E_h^{-1}$	$=$	1.648778×10^{-41} C² m² J⁻¹
Frequency ω		$1\ E_h$	$=$	219474.63067 cm⁻¹

The conversion factors have been derived from fundamental constants supplied in Cohen and Taylor [1]. In the present thesis, all internuclear distances have been quoted in angstroms (1 Å = 1 × 10⁻¹⁰ m) and all electrical properties have been reported in Hartree atomic units. The abbreviation au is used throughout the thesis in place of the atomic unit symbols of a_0, ea_0, etc. and corresponds to the relevant atomic units for the property.

Appendix II. Atomic masses

Table AII.1.
Isotopic masses for the most abundant isotopes of the first and second-row atoms and deuterium.[a]

Isotope	Mass / amu	Isotope	Mass / amu
^{1}H	1.007825	^{2}H (D)	2.014102
^{12}C	12.000000	^{28}Si	27.97693
^{14}N	14.003074	^{31}P	30.97376
^{16}O	15.994915	^{32}S	31.97207
^{19}F	18.99840	^{35}Cl	34.96885

[a] Nuclear masses from [2].

Appendix III. Optimized theoretical geometries

All bond lengths r are in angstroms (Å), all bond angles θ are in degrees (°).

Table AIII.1.
Optimized TZPOL1 theoretical r_e geometries for the second-row hydrides

	Parameter	SCF	MP2
SiH$_4$	r_{SiH}	1.4788741	1.4794946
PH$_3$	r_{PH}	1.4077317	1.4128082
	θ_{HPH}	95.4552	93.3871
H$_2$S	r_{SH}	1.3296268	1.3365276
	θ_{HSH}	94.0917	91.9930
HCl	r_{HCl}	1.2676277	1.2745320

Table AIII.2.
Optimized theoretical r_e geometries for the fluoromethanes

Theory / Basis Set	Molecular Parameters			
CF$_4$		r_{CF}		
SCF/DZP–ANO4		1.3053574		
MP2/DZP–ANO4		1.3359283		
SCF/DZP–ANO2		1.2997411		
MP2/DZP–ANO2		1.3263029		
B3LYP/cc-pVTZ		1.3259175		
CHF$_3$	r_{CH}	r_{CF}	θ_{HCF}	
SCF/DZP–ANO2	1.0777879	1.3162354	110.4243	
MP2/DZP–ANO2	1.0889446	1.3433652	110.5090	
B3LYP/cc-pVTZ	1.0895275	1.3399308	110.4208	
CH$_2$F$_2$	r_{CH}	r_{CF}	θ_{FCF}	θ_{HCH}
SCF/DZP–ANO2	1.0812087	1.3405437	108.2556	112.9869
MP2/DZP–ANO2	1.0916439	1.3693402	108.3433	113.9752
B3LYP/cc-pVTZ	1.0909078	1.3609276	108.6523	113.1839
CH$_3$F	r_{CH}	r_{CF}	θ_{HCF}	
SCF/DZP–ANO2	1.0834371	1.3712564	108.7061	
MP2/DZP–ANO2	1.0925425	1.4020413	108.4751	
B3LYP/cc-pVTZ	1.0905393	1.3872476	109.0370	

Table AIII.3.
Optimized theoretical r_e geometries for C_2H_4.

Theory / Basis Set	r_{CC}	r_{CH}	θ_{HCH}
SCF/DZP–ANO2	1.3270262	1.0765678	116.8883
MP2/DZP–ANO2	1.3556792	1.0859647	117.4550

Table AIII.4.
Optimized theoretical r_e geometries for C_2H_6.

Theory / Basis Set	r_{CC}	r_{CH}	θ_{HCH}
Staggered			
SCF/DZP–ANO2	1.5313901	1.0869166	107.7165
SCF/DZP–ANO3	1.5256177	1.0863423	107.7097
MP2/DZP–ANO2	1.5393552	1.0945218	107.6307
MP2/DZP–ANO3	1.5267047	1.0912300	107.6613
Eclipsed			
MP2/DZP–ANO3	1.5405890	1.0902463	107.1913

Appendix IV. MP2-ANO basis set exponents and contraction coefficients

The substrates used for the MP2-ANO basis set are the triple-zeta valence (TZV) substrates of Schäfer *et al.* [3, 4]. All exponents in the following Tables are in atomic units. The *s*-type exponents for the hydrogen substrate were scaled by $(1.25)^2$ for molecular calculations. The MP2-ANO basis set is summarised as follows:

Atom	Substrate	Augmenting functions	MP2-ANO set
H	(6*s*) / [3*s*]	1*s*3*p*1*d*	4*s*3*p*1*d*
B-Ne	(11*s*6*p*) / [5*s*3*p*]	1*s*1*p*3*d*1*f*	6*s*4*p*3*d*1*f*
Al-Ar	(14*s*8*p*) / [5*s*4*p*]	1*s*1*p*3*d*1*f*	6*s*5*p*3*d*1*f*

The MP2-ANO basis set augmenting function exponents and contraction coefficients for the atoms H, C-Ne, Si-Ar are supplied in the following tables.

Table AIV.1.
MP2-ANO [4*s*3*p*1*d*] basis set augmenting functions for the Hydrogen atom

Hydrogen H		Contraction coefficients		
Type	Exponents	1	2	3
s	0.039469	-0.99373463		
	0.011081	0.11176533		
p	1.407000	-0.55217858	-0.06532398	-0.58243112
	0.388000	-0.79306547	0.01156039	-0.79330120
	0.102000	-0.25643584	-0.99350833	-0.16071049
	0.026814	-0.01966303	-0.09241392	0.07496226
d	1.057000	0.05578148		
	0.247000	-0.99844300		

Table AIV.2.
MP2–ANO [6s4p3d1f] basis set augmenting functions for the Carbon atom

Carbon C		Contraction coefficients		
Type	Exponents	1	2	3
s	0.044020	0.83000701		
	0.020362	0.55775296		
p	0.035690	0.99080033		
	0.012666	0.13533182		
d	1.097000	−0.15364934	−0.14754986	−0.02692912
	0.318000	−0.98700254	−0.80937850	0.96654596
	0.100000	−0.04079651	−0.48101293	0.24432649
	0.031447	−0.02352674	−0.30292251	0.07326866
f	0.761000	0.47909452		
	0.263000	0.87776331		

Table AIV.3.
MP2–ANO [6s4p3d1f] basis set augmenting functions for the Nitrogen atom

Nitrogen N		Contraction coefficients		
Type	Exponents	1	2	3
s	0.057600	−0.98899213		
	0.024310	−0.14796814		
p	0.049100	−0.99793633		
	0.016905	−0.06421120		
d	1.654000	0.18591827	0.15988843	0.10353116
	0.469000	0.98248959	0.84416963	−0.95318403
	0.151000	0.00680609	0.46461876	−0.27715280
	0.048616	0.01011291	0.21434257	−0.06251260
f	1.093000	−0.41968436		
	0.364000	−0.90767011		

Table AIV.4.

MP2–ANO [6s4p3d1f] basis set augmenting functions for the Oxygen atom

Oxygen O		Contraction coefficients		
Type	Exponents	1	2	3
s	0.073760	−0.99602808		
	0.029401	−0.08903972		
p	0.059740	−0.99995084		
	0.020419	0.00991504		
d	2.314000	0.21752187	−0.16400361	0.05278016
	0.645000	0.97582705	−0.83654306	−0.94525115
	0.214000	0.01629595	−0.46572968	−0.31592453
	0.071002	0.01342521	−0.23747503	−0.06249966
f	1.428000	−0.27567843		
	0.500000	−0.96124992		

Table AIV.5.

MP2–ANO [6s4p3d1f] basis set augmenting functions for the Fluorine atom

Fluorine F		Contraction coefficients		
Type	Exponents	1	2	3
s	0.091580	−0.99859699		
	0.034905	−0.05295327		
p	0.073610	0.99627133		
	0.025026	0.08627530		
d	3.107000	0.24923983	−0.15083472	−0.10384029
	0.855000	0.96796652	−0.76448272	0.93201379
	0.292000	−0.02519110	−0.55697518	0.33750296
	0.099724	0.01690346	−0.28739120	0.08160413
f	1.917000	−0.05669030		
	0.724000	0.99839181		

Table AIV.6.

MP2–ANO [6s4p3d1f] basis set augmenting functions for the Neon atom

Neon Ne		Contraction coefficients		
Type	Exponents	1	2	3
s	0.113300	−0.99944631		
	0.042465	−0.03327264		
p	0.091750	0.97985671		
	0.031638	0.19970186		
d	4.014000	0.26785510	0.13322122	−0.08199158
	1.096000	0.96010210	0.68265087	0.91601787
	0.386000	−0.06906712	0.61031372	0.38184428
	0.135945	0.04107720	0.37915307	0.09156200
f	2.544000	−0.74561629		
	1.084000	−0.66637553		

Table AIV.7.

MP2–ANO [6s5p3d1f] basis set augmenting functions for the Silicon atom

Silicon Si		Contraction coefficients		
Type	Exponents	1	2	3
s	0.033000	0.95969915		
	0.012707	0.28102942		
p	0.023700	0.97632133		
	0.008018	−0.21632538		
d	0.481000	−0.55124687	0.12988255	−0.28191444
	0.159000	−0.69411767	−0.76044824	−0.56893264
	0.055600	−0.44710395	−0.61191148	0.69775305
	0.019443	−0.12010662	−0.17439421	0.33163321
f	0.336000	0.96420807		
	0.125000	0.26514674		

Table AIV.8.

MP2–ANO [$6s5p3d1f$] basis set augmenting functions for the Phosphorus atom

Phosphorus P		Contraction coefficients		
Type	Exponents	1	2	3
s	0.040900	−0.99230471		
	0.014651	−0.12381987		
p	0.030700	0.97577871		
	0.010431	−0.21875994		
d	0.652000	0.49343787	−0.20015889	0.27155059
	0.216000	0.75125126	0.81531331	0.33911304
	0.077500	0.42920297	0.53131336	−0.84835656
	0.027807	0.08902484	0.11360780	−0.30257855
f	0.452000	0.95649090		
	0.165000	0.29176215		

Table AIV.9.

MP2–ANO [$6s5p3d1f$] basis set augmenting functions for the Sulfur atom

Sulfur S		Contraction coefficients		
Type	Exponents	1	2	3
s	0.049700	0.99733982		
	0.016976	0.07289232		
p	0.035100	−0.98834075		
	0.011439	0.15225818		
d	0.819000	0.70105306	−0.36097077	−0.14720866
	0.269000	−0.64817977	−0.93234150	−0.86590647
	0.101000	0.29008234	0.02083307	−0.44037927
	0.037922	0.06511393	−0.00232819	−0.18601529
f	0.557000	0.94549016		
	0.218000	0.32565067		

Table AIV.10.

MP2–ANO [6s5p3d1f] basis set augmenting functions for the Chlorine atom

Chlorine Cl		Contraction coefficients		
Type	Exponents	1	2	3
s	0.059100	0.99899690		
	0.019445	0.04477948		
p	0.041900	−0.98910255		
	0.013433	0.14722818		
d	1.046000	−0.35742214	0.28398384	0.23515799
	0.344000	−0.82320522	−0.85626525	0.18822098
	0.135000	−0.42913575	−0.41834147	−0.89571102
	0.052980	−0.10210335	−0.10560968	−0.32707087
f	0.706000	−0.94072149		
	0.312000	−0.33918002		

Table AIV.11.

MP2–ANO [6s5p3d1f] basis set augmenting functions for the Argon atom

Argon Ar		Contraction coefficients		
Type	Exponents	1	2	3
s	0.068500	−0.99979121		
	0.021672	−0.02043363		
p	0.048700	−0.99269480		
	0.015043	0.12065250		
d	1.254000	0.31064717	0.54265593	0.22127635
	0.410000	0.85034168	0.76428837	−0.87424772
	0.169000	0.40995922	−0.34736769	−0.41706657
	0.069661	0.11113415	−0.02689818	−0.11306268
f	0.890000	−0.95150822		
	0.406000	−0.30762333		

TZP–ANO1 basis set

The TZP–ANO1 [$6s6p4d1f$]/[$4s3p1d$] basis set used in the second-row hydrides study (Chapter 4) was constructed using the MP2–ANO basis set for hydrogen and the following recipe for second-row atoms :

1. For the appropriate atom a d-type function, with exponent supplied below, was added to the MP2–ANO [$6s5p3d1f$] basis set.

Si	1.455101
P	1.968074
S	2.493535
Cl	3.180570

2. The p-type diffuse functions were uncontracted.

DZP–ANOx basis sets

The DZP–ANO basis set was constructed from the double-zeta (DZ) Thakkar *et al.* substrate [5] and the MP2–ANO polarization functions in the Tables below. The method for obtaining the relevant DZP–ANOx sets, where x is the number of d-type polarization functions, is given below:

- For DZP–ANO3, the f-type function was deleted from DZP–ANO.
- For DZP–ANO2, the number (3) d-type function was deleted from DZP–ANO3.
- For DZP–ANO2(f), the number (3) d-type function was deleted from DZP–ANO.
- For DZP–ANO1, the number (1) and (3) d-type functions were deleted from DZP–ANO3.

The basis set for hydrogen was constructed from the Thakkar *et al.* double-zeta (DZ) substrate and augmenting functions with exponents and contraction coefficients (italicised) given below:

s	0.025260
p	(*0.5*, 1.407, *0.5*, 0.388)
p	(*0.5*, 0.150568, *0.5*, 0.077927)

Appendix V. Publications

(i) Russell, A.J. and Spackman, M.A., *"Vibrational averaging of electrical properties. Development of a routine theoretical method for polyatomic molecules"*, Molecular Physics, **84**, 1239 (1995).

(ii) Russell, A.J. and Spackman, M.A., *"Accurate ab initio study of Acetylene. Vibrational and rotational corrections to electrical properties"*, Molecular Physics, **88**, 1109 (1996).

(iii) Russell, A.J. and Spackman, M.A., *"An ab initio study of vibrational corrections to the electrical properties of the second-row hydrides"*, Molecular Physics, **90**, 251 (1997).

References

[1]   Cohen, E. R., and Taylor, B. N., 1987, *J. Res. Natl. Bur. Stand.*, **92**, 85.

[2]   Lide, D. R., 1991, *CRC Handbook of Chemistry and Physics* (CRC Press).

[3]   Schäfer, A., Horn, H., and Ahlrichs, R., 1992, *J. chem. Phys.*, **97**, 2571.

[4]   Schäfer, A., Huber, C., and Ahlrichs, R., 1994, *J. chem. Phys.*, **100**, 5829.

[5]   Thakkar, A. J., Koga, T., Saito, M., and Hoffmeyer, R. E., 1993, *Int. J. Quantum Chem. Quantum chem. Symp.*, **27**, 343.